

# Methods for Obtaining and Reducing Experimental Droplet Impingement Data on Arbitrary Bodies

Michael Papadakis\*

Wichita State University, Wichita, Kansas 67208

and

R. Elangovan,† George A. Freund Jr.,‡ and Marlin D. Breer§

Boeing Company, Wichita, Kansas 67227

Experimental water droplet impingement data are used to validate particle trajectory computer codes used in the analysis and certification of aircraft de-icing/anti-icing systems. Water droplet impingement characteristics of aerodynamic surfaces are usually obtained from wind-tunnel dye tracer experiments. This paper presents a dye tracer method for measuring water droplet impingement characteristics on arbitrary geometries and a new data reduction method, based on laser reflectance measurements, for extracting impingement data. Extraction of impingement data has been a very time-consuming process in the past. The new data reduction method developed is at least an order of magnitude more efficient than the method previously used. The accuracy of the method is discussed and results obtained are presented.

## Nomenclature

|            |   |
|------------|---|
| AVS        | = average surface distance, cm  |
| $d$        | = particle diameter, $\mu\text{m}$  |
| $g$        | = gravitational acceleration, $\text{m/s}^2$  |
| He-Ne      | = helium-neon gas laser   |
| HIGHLIGHT  | = leading edge of a given geometry  |
| LWC        | = liquid water content of spray cloud, $\text{g/m}^3$   |
| MVD        | = mean volumetric diameter of the droplet cloud, $\mu\text{m}$ ; the diameter for which half of the total liquid water content is contained in droplets larger than the mean and half in droplets smaller than the mean |
| $V_\infty$ | = freestream velocity, mph  |
| $\alpha$   | = angle of attack, deg  |
| $\beta$    | = local impingement efficiency for clouds with nonuniform droplet size  |
| $\mu$      | = absolute air viscosity, $\text{kg/ms}$  |
| $\rho$     | = particle density, $\text{kg/m}^3$   |

## Introduction

ICE accumulation on aircraft surfaces can severely alter the aerodynamic characteristics of the aircraft and degrade both aircraft performance and safety. To maintain aerodynamic surfaces free of ice, de-icing or anti-icing systems are employed on aircraft that may be exposed to icing conditions. The design of cost-effective ice removal (de-icing) and ice prevention (anti-icing) systems requires knowledge of the water droplet impingement characteristics of aircraft surfaces that must be protected from ice accretion.

A body flying through a cloud of droplets will not, in general, intercept all of the droplets originally directly ahead of its frontal area. The total and local accumulation of droplets on the body surface and the limits of droplet impingement depend on a number of factors. These factors include

body size and shape, freestream velocity, body orientation, air density and viscosity, liquid water content (LWC), droplet size, droplet distribution, and droplet density.

A number of computer programs are currently available for predicting impingement characteristics of internal and external surfaces for two-dimensional, axisymmetric, and three-dimensional geometries. These codes, however, require extensive validation against experimental data before they can be applied to the design and analysis of aircraft de-icing/anti-icing systems.

Experimental droplet impingement data for two-dimensional and axisymmetric bodies at small angles of attack were obtained during the late 1940s and early 1950s<sup>1-4</sup> by the National Advisory Committee for Aeronautics (NACA). Wind-tunnel droplet impingement tests were conducted on cylinders, airfoils, and bodies of revolution. A dye tracer technique was developed by von Glahn et al.<sup>1</sup> to obtain the impingement characteristics of a body exposed to a cloud of droplets. In this technique, water containing a small amount of water-soluble dye was injected in the form of droplets into the airstream ahead of the body by means of spray nozzles. Thin strips of moisture absorbing (blotter) paper were wrapped around the leading edges of the test geometry to collect the spray. A permanent trace of dye was obtained on the blotter strips when the body was exposed to the droplet cloud. The limits of impingement were obtained directly from the rearmost dye trace on the absorbent material. The amount of dye per unit area obtained in a measured time interval was determined by colorimetric analysis. Several hours were required to reduce the data from a single blotter strip. Although this process was sufficiently accurate, its application to configurations requiring multiple tests and a large number of blotter strips for each test was not practical.

The experimental water droplet impingement data produced by the NACA group were limited to configurations of interest to the aviation community in the 1940-1955 time period. A small amount of engine inlet data was also obtained by the NACA group, but these data generally do not apply to modern subsonic engine inlets. To validate trajectory codes applied to icing analysis of modern engine inlets and modern wing geometries, additional experimental trajectory data were required by the icing research community.

The objective of the present work was to establish an experimental water droplet impingement data base for an extensive range of modern inlet and wing geometries. More specifically, the research objectives were as follows.

Presented in part as Paper 86-0406 at the AIAA 24th Aerospace Sciences Meeting, Reno, NV, Jan. 6-9, 1986; received April 5, 1989; revision received July 28, 1990; accepted for publication Aug. 1, 1990. Copyright © 1990 by the American Institute of Aeronautics and Astronautics, Inc. All rights reserved.

\*Assistant Professor, Aerospace Engineering Department. Member AIAA.

†Senior Specialist Engineer. Member AIAA.

‡Senior Specialist Engineer.

§Senior Principal Engineer. Member AIAA.

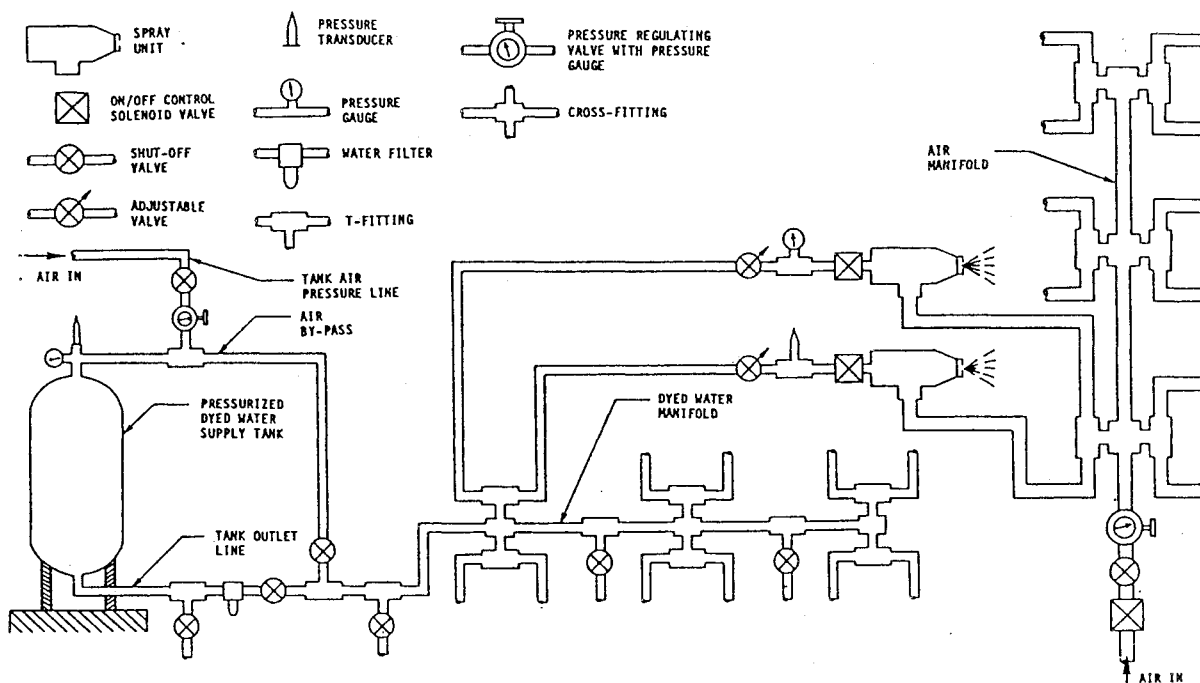


Fig. 1 Schematic of spray system.

1) To develop an efficient and accurate data reduction method for extracting the impingement data from the blotter strips.

2) To automate the data reduction process so that large numbers of blotter strips can be reduced in a relatively short time.

3) To validate the data reduction technique.

4) To develop an extensive data base for modern aircraft surfaces, particularly for engine inlets, for which very little data was available.

5) To correlate experimental data with analysis results from trajectory computer codes.

The current series of impingement tests were conducted at the NASA Lewis Icing Research Tunnel (IRT). These tests encompassed a wide variety of models and test conditions and were performed in September 1985 and in April 1989. The impingement data obtained in 1985 can be found in Ref. 5 and include results for a 4-in.-diam cylinder, a 13-in. chord NACA 65<sub>2</sub>015 airfoil section, a 36-in. chord MS (1)-0317 airfoil section, an axisymmetric engine inlet, a Boeing 737-300 engine inlet, and three ice shapes. The complete 1989 test results for a NLF-0414F airfoil section, a swept MS(1)-0317 airfoil, a swept NACA 0012 wingtip, a Boeing 737-300 engine inlet, a Boeing 747 engine inlet, and two ice shapes will be made available in a future publication.

The emphasis in this paper is the description of the experimental and data reduction methods. The repeatability and accuracy of these methods is discussed in detail. Experimental impingement data obtained for a 4-in. cylinder and a NACA 65<sub>2</sub>015 are also presented and are compared with analytical data.

## Experimental Method

### Dye Tracer Technique

The dye tracer technique used in the present water droplet impingement tests is similar to the one developed by NACA in the 1950s. The main differences between these two methods are in the measurement of cloud liquid water content and droplet size and distribution. The type of dye and blotter paper used in the present method are also different from the ones used by NACA. Some of these differences were required for the new data reduction method, whereas others were made to improve the accuracy of the experimental data.

### Test Facility

All tests were conducted in the NASA Lewis Icing Research Tunnel, which has a 6-ft  $\times$  9-ft-wide  $\times$  20-ft-long test section and a maximum airspeed of 300 mph. The tests were performed at a tunnel air temperature of approximately 50°F and at airspeeds ranging from 165–175 mph.

### Test Procedure

Prior to the impingement tests, a number of steps were performed to prepare the IRT for testing. The specially designed spray system was installed and the locations of the various nozzles were adjusted to produce a uniform cloud. With the test model removed, a device called "the collector" was employed to measure the local LWC at each blotter strip location and for every spray and tunnel condition. This was done to account for any cloud nonuniformity that existed after the final spray nozzle adjustment. In addition, the mass flow measurement system required for engine inlet testing was calibrated.

Following these adjustments and measurements, the impingement tests were performed. Each model was installed in the tunnel test section, blotter strips were attached at the locations of interest, the tunnel was brought up to speed, and the spray system was activated. Spraying times varying from 3 to 5 s, depending on cloud droplet size, were sufficiently long for producing a dye trace on the blotter strips. The blotter strips were stored for analysis, the model was cleaned, and new blotter strips were applied for the next test condition. The procedure was repeated 3–5 times at each test point to obtain a statistical average. Details of the various aspects of the dye tracer technique are given below.

### Spray System

To avoid blotter paper saturation, the spray time was kept very short. The IRT spray system could not produce stable sprays for such short durations and could not be turned off and on quickly. Thus, a new spray system was designed and built. This system consisted of a pressurized tank which contained the dye solution and 12 nozzle fixtures. The nozzle fixtures were mounted on the IRT spray bars located in the tunnel plenum chamber. A schematic of the spray system is shown in Fig. 1.

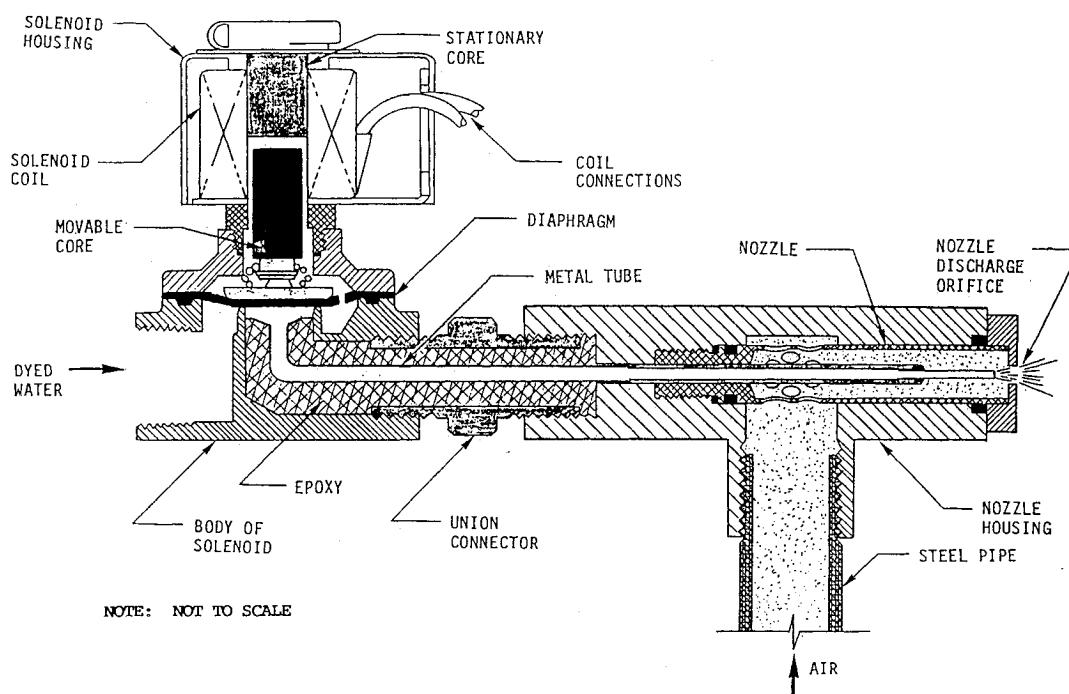


Fig. 2 Cross section of spray nozzle.

Each nozzle fixture consisted of a standard IRT spray nozzle, a nozzle housing where hoses carrying pressurized air and dye solution were attached, a solenoid valve for turning off and on the dye supply, and pressure gauges for monitoring the pressure of the dye solution at the nozzle entry. To keep system response as fast as possible, the volume of the nozzle housing downstream of the solenoid valve was minimized, as shown in Fig. 2.

Spray clouds of different droplet sizes were produced by varying the ratio of air-to-dyed water supply pressures. Two supply pressures were used for air, 65 psig and 80 psig. The dyed water pressure was maintained at 100 psig at each spray nozzle.

#### Dye Solution and Blotting Paper

The following requirements for the dye determined its selection for the current impingement tests:

- 1) safe to use and easy to clean off the tunnel walls and model surface;
- 2) highly water soluble;
- 3) stable with respect to light and temperature for long periods of time, and it must not react chemically with components of the spray system; and
- 4) highly absorbing at 632.8 nm, which is the wavelength of a readily available red He-Ne laser (such a laser was later used in the data reduction system).

A dye that was found to satisfy all of these conditions is a Brilliant Blue No. 1 food color dye. The dye concentrations chosen for the tests were 0.0005% by weight for the 1985 tests and 0.0002% by weight for the 1989 tests. These concentrations combined with the short spray times produce dye traces that are neither too dark nor too light for the reflectance method used to reduce the data. The lower concentration used in the 1989 tests resulted in dye traces with color intensities closer to the optimum required to maximize the accuracy of the data reduction method.

The selection of blotter paper was based on the following properties.

- 1) The paper must be able to absorb dyed water without becoming easily saturated.
- 2) The thickness of the material must be small so that it does not affect the aerodynamic characteristics of the model,

and it must be readily formed to follow the body contour without breaking.

- 3) The consistency of the paper properties, particularly its reflectance, must be nearly constant.

Several types of blotter paper were tested, and the paper that was found to work well with the present experimental and data reduction techniques was the James River No. 100 Veri-good Blotting Paper. A sufficient quantity of this paper, manufactured in a single lot, was obtained for the present tests.

#### Uniformity Test

A uniform distribution of the spray cloud throughout the wind-tunnel test section is highly desirable, particularly when average LWC measurements are used to reduce the data. The test section of the NASA Lewis IRT is 6 ft × 9 ft, so a very large number of nozzles is required to produce a uniform spray cloud over this area. However, the area over which all the impingement measurements were made was 2 ft × 3 ft, so 12 nozzles were sufficient to produce a uniform cloud. A large number of uniformity runs were performed during which the 12 nozzles of the spray system were adjusted vertically and horizontally until the variation in LWC was  $\pm 10\%$  from the average value in the 2-ft × 3-ft test area.

Cloud uniformity was measured using a 6-ft × 9-ft brass grid with horizontal and vertical increments 6 in. apart. Blotter strips were attached to this grid to cover an area of 2 ft × 3 ft centered about the tunnel longitudinal axis, as shown in Fig. 3. The tunnel was brought up to test speed, and the blotters were sprayed. The dye distribution on each blotter (35 blotter strips were used during each test) was determined using the data reduction method, and the nozzles were adjusted to remove dark or light regions of dye distribution.

#### Droplet Size and Distribution

Validation of computer trajectory codes requires knowledge of droplet diameter and distribution. Droplet size and distribution for the spray system pressure ratios ( $P_{\text{air}}/P_{\text{water}}$ ) used in the present trajectory tests were provided by NASA Lewis. Two spray clouds with MVDs of 16  $\mu\text{m}$  and 20  $\mu\text{m}$  were used. The corresponding spray system pressure ratios for these droplet sizes were (80 psig<sub>air</sub>/100 psig<sub>water</sub>) and (65 psig<sub>air</sub>/100

psig<sub>water</sub>), respectively. Details of droplet sizes and distributions are given in Ref. 5.

#### Local LWC Measurement

Local water droplet impingement efficiency  $\beta$  for a body is expressed as the ratio of local flux normal to the surface ( $LWC_{\text{surface}} \times V_{\text{normal}}$ ) divided by the freestream flux ( $LWC \times V_{\infty}$ ). For a cloud with uniform LWC, an average LWC value can be used. This average value is usually obtained by measuring LWC at a given location. Uniform wind-tunnel spray clouds with variations in cloud LWC of less than  $\pm 10\%$  are very difficult to obtain over large areas. Thus, for maximum accuracy, LWC values must be obtained at all locations where the actual impingement measurements are made.

In the NACA tests, an aspirating device was used to measure LWC. This device consisted essentially of a tube that sucked in the approaching air and cloud droplets at the freestream velocity (inlet velocity ratio, 1.0). Thus, both the air streamlines and droplets entered the tube along straight paths. All of the dyed droplets were deposited on a filter mounted within the tube, leaving a dye trace that was analyzed colorimetrically, as described in Ref. 1. The LWC measurements were made at only one location for each spray cloud.

The aspirating device method was not considered practical for simultaneous measurements of LWC at various locations within the tunnel section. Thus, a new device, referred to as the "collector mechanism," was designed for measuring local LWC. The LWC was measured by a small wedge-shaped blade ("the collector") mounted on the mechanism, as shown in Fig. 4a. The maximum number of collector blades used at any one time was nine (eight circumferentially and one in the middle). The size of the wedge is small (0.2 in. wide, approximately 4 in. long and 1 in. in chord) to minimize disturbance to the flow. This enables the device to collect most of the water droplets traveling within its projected area. Details of a single blade are shown in Fig. 4b.

Theoretical impingement efficiencies for the collector were determined for the MVDs and spray cloud distributions discussed above using the method described in Ref. 6. In this method, the flowfield about the collector is obtained by solving the compressible stream function equation numerically. The droplet trajectories are then obtained by solving the system of differential equations governing the motion of the droplet. These equations are as follows:

$$\frac{dU_x}{dt} = Cd_{Rv} Rv \frac{(V_x - U_x)}{24P} \quad (1)$$

$$\frac{dU_y}{dt} = Cd_{Rv} Rv \frac{(V_x - U_x)}{24P} - (1 - w) \frac{gC}{V_{\infty}^2} \quad (2)$$

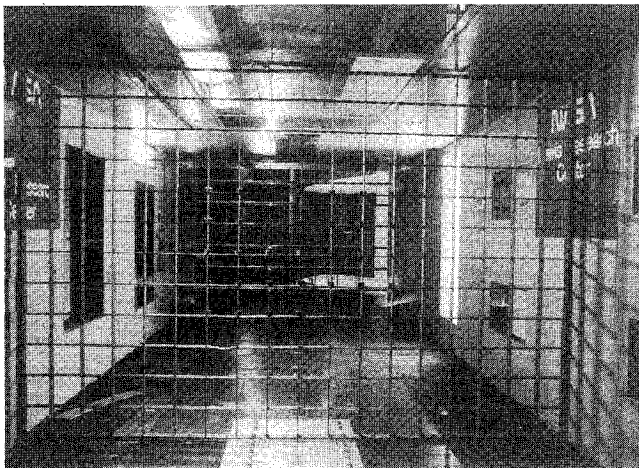


Fig. 3 Grid with blotter squares installed in the IRT test section (looking upstream).

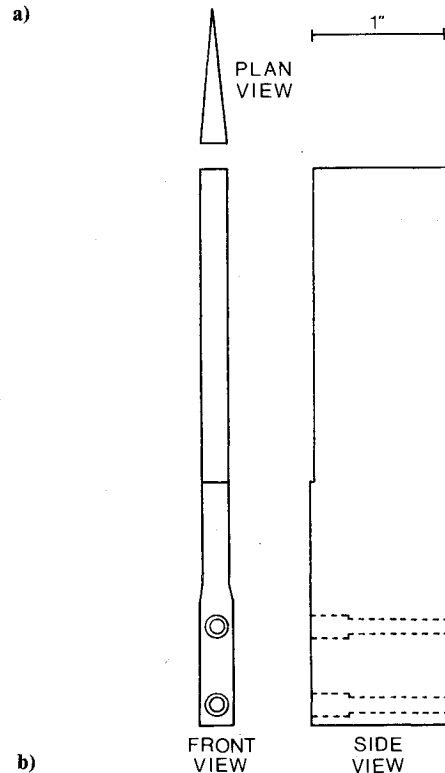
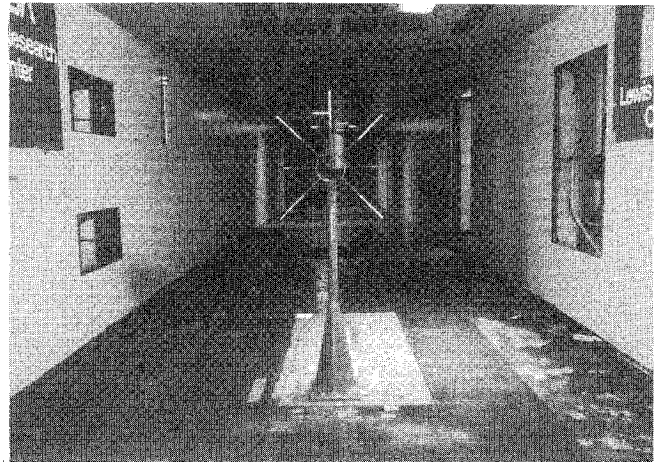


Fig. 4 Collector mechanism: a) nine-blade mechanism used in all 1989 tests (only 6 blades are shown), b) details of a collector blade.

$$\frac{dx}{dt} = U_x \quad (3)$$

$$\frac{dy}{dt} = U_y \quad (4)$$

In these equations,  $Cd_{Rv}$  is the drag coefficient of the spherical particle based on the particle Reynolds number  $Rv$ ;  $P = \rho V_{\infty} d^2 / (18\mu C)$  is the inertia parameter of the particle;  $t$  is the time (dimensionless with  $C/V_{\infty}$ );  $w$  is the density ratio of air to particle;  $C$  is the characteristic dimension of body;  $Rv = R_{\infty} |(V - U)|$  is the relative Reynold's number of the particle;  $U_x$  and  $U_y$  are the particle velocity components (dimensionless with  $V_{\infty}$ );  $V_x$  and  $V_y$  are the air velocity components (dimensionless with  $V_{\infty}$ ); and  $x$  and  $y$  are the components of the particle position vector (dimensionless with  $C$ ).

The analytical results for the collector impingement efficiency were obtained using discrete representations of the measured droplet distributions. Each discrete distribution consisted of seven particle sizes. Figure 5 gives the theoretical efficiency of the collector for the spray cloud with an MVD of

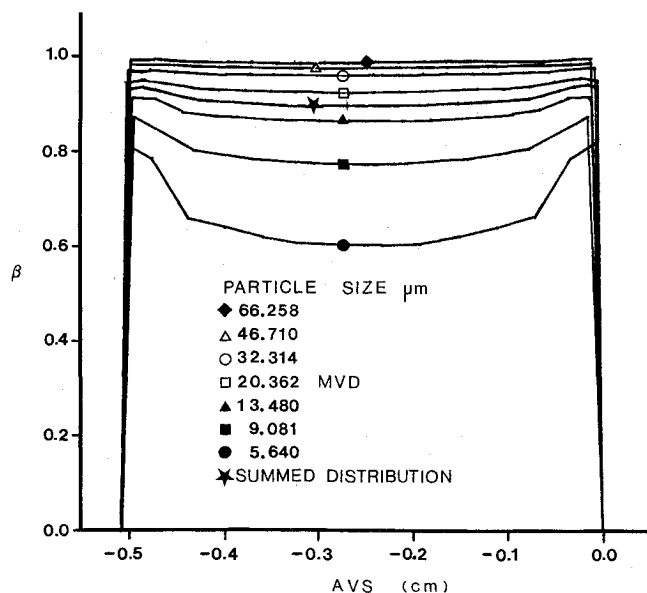


Fig. 5 Local impingement efficiency  $\beta$  of the collector as a function of surface distance.

20  $\mu m$ . Eight curves are shown in this figure, one for each of the seven particle sizes and one for the summed distribution. The summed distribution is used to determine the efficiency of the collector. For the MVD of 20  $\mu m$ , the efficiency of the collector is 0.89%.

After testing a given model, the collector was positioned close to the location where each blotter strip on the model had been installed and was exposed to the spray cloud under identical tunnel conditions as the model itself. Test models with blotter strips installed at two locations, for example, required LWC measurements for each of these two locations. A rectangular blotter strip (0.2 in.  $\times$  1.5 to 2 in.) mounted on the wedge was used to collect dye during each LWC test. Spray times for the collector were identical to the spray times used for the model.

The collector mechanism shown in Fig. 4a was used with all 1989 tests. Similar devices with one and four blades were used in 1985. The newer version allowed more local LWC data to be collected for the engine inlet models.

### Data Reduction Method

#### NACA Data Reduction Method

The dyed blotter strips obtained during the 1950s' tests were typically 3 in. wide  $\times$  7 in. long. These blotters were segmented into  $\frac{1}{8}$   $\times$  1.5-in. ribbons, and the dye was dissolved out of each segment by adding a known amount of distilled water. The weight of dye in this solution was determined by the amount of light of a suitable wavelength transmitted

through the solution by use of a calibrated colorimeter (Ref. 1). For a given dye concentration (generally 0.5–1.0% by weight), the quantity of water deposited was easily calculated once the amount of dye on each ribbon was found.

The NACA method was accurate and was probably the only practical way for reducing the data, considering the technology available in the 1950s. This method, however, had a number of disadvantages:

- 1) Cutting each ribbon into segments and dissolving the dye out of each segment was very laborious and time consuming.
- 2) The blotter strips were destroyed during the reduction process.
- 3) The resolution of the reduction method was limited to the size of each blotter segment, which had to be large enough so that a measurable quantity of dye could be extracted. Typically five to six data points were obtained per inch of the dyed blotter paper.

#### Laser Reflectance Method

In the present data reduction method, impingement data are extracted by scanning each blotter paper with a red He-Ne laser beam. This method is based on the assumption that the surface reflectance of the dyed paper is a measure of the dye mass per unit area of the paper. Dyed regions on the blotter strip corresponding to high droplet impingement rates are darker in color and reflect less light. The opposite is true for areas on the blotter corresponding to low impingement rates. Regions with no dye accumulation are white and reflect the maximum amount of laser light. The relation between dye concentration and reflectance is not linear and is determined from calibration tests. Once the amount of dye on the paper is found using the laser reflectance technique, the amount of water deposited is determined from the dye concentration in the spray solution used in the test.

To maximize the sensitivity of the reflectance method, the dye used in the tests must have a strong absorption at the wavelength of the laser radiation. This is accomplished by using a blue dye whose maximum absorption occurs at 629.5 nm, which is very close to the wavelength (632.8 nm) of the red He-Ne laser employed in the data reduction system.

#### Method Development

Reflection from most real surfaces is a combination of specularly (mirror-like) and diffusely reflected light. The blotter paper used in these tests is primarily a diffused reflector. The diffuse reflectance of a nonabsorbing mat surface can be expressed by

$$R = (I_0/\pi) \cos \alpha \cos \theta \quad (5)$$

where  $I_0$  is the maximum intensity of the diffusely reflected light at normal incidence,  $\alpha$  is the angle of incidence, and  $\theta$  is the angle of observation.<sup>7</sup> For a given  $\alpha$ , the maximum value of  $R$  occurs in the direction normal to the paper, i.e.,  $\theta = 0$

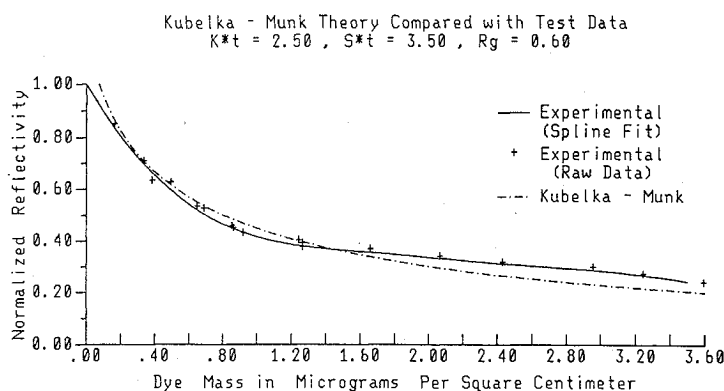


Fig. 6 Standard normalized reflectivity calibration curve.

deg. In addition, small values of  $\alpha$  with respect to the normal increase the value of  $R$ . To maximize the light reflected from the blotter paper and, thus, enhance the sensitivity of the laser reflectometer, the incident laser beam was set at 10 deg from the normal to the paper, and the diffusely reflected light was collected in the near normal direction ( $\theta = 0$  deg).

A theory which is often used to describe diffuse reflectance is that of Kubelka-Munk.<sup>8,9</sup> In this theory, the intensity of the transmitted beam  $I$  and the intensity of the reflected beam  $J$  are governed by the following ordinary differential equations:

$$-\frac{dI}{dx} = -(S + K)I + SJ \quad (6)$$

$$\frac{dJ}{dx} = SI - (S + K)J \quad (7)$$

In these equations the two parameters  $S$  and  $K$  are the scattering and absorption coefficients per unit thickness of the reflector material. The distance traveled by the light within the reflector material is denoted by  $x$ . The Kubelka-Munk theory in its basic form applies to two collimated beams of monochromatic light propagating normal to the surface of the material (dyed blotter paper). This theory, however, can be extended to describe a diverging beam incident on a surface at an arbitrary angle.

The extended theory of Kubelka-Munk for diffuse reflection was used as a guide in developing the present data reduction method. The theory is approximately correct as long as the light source is monochromatic, and the reflections and absorptions occur at infinitesimal distances within the paper and are constant over the area illuminated by the beam at the penetration depth. In addition, the diffuse reflector must have uniform optical properties. With these assumptions and with appropriate boundary conditions, the preceding differential equations can be integrated for the case of a layer (blue dye) of finite thickness  $t$  deposited onto a substrate (blotter paper) to provide the following expression for the reflectivity of the two component material:

$$R = \frac{1 - R_g [A - B \coth(BSt)]}{A + B \coth(BSt) - R_g} \quad (8)$$

where  $R_g$  is the reflectance of the blotter paper,  $A = (S + K)/S$ , and  $B = \sqrt{A^2 - 1}$ . This expression for  $R$  was used as a reference during the development of the laser calibration curve.

### Calibration of Laser Reflectance Method

To extract the experimental water droplet impingement data from the dyed blotter strips, a calibration curve was produced. This curve relates laser reflectance to dye mass on the blotter strip. The curve is a standard against which the reflectance of each blotter strip is compared during the data reduction process. If the type of dye, the blotter paper, and the laser instrumentation remain constant the curve does not change.

To produce the laser reflectance calibration curve, a series of tests was performed. In these tests a number of blotter paper samples were uniformly impregnated with dye solutions of known concentrations. Care was exercised not to saturate the blotters and to keep the dye penetration into the blotter as low as possible. These tests produced blotter strips with color intensities covering the range of interest. From each colored blotter sample, three disks of 1 in. in diameter were cut (a total of 54 disks were produced), and the reflectance of each disk was recorded. The dye from each disk was extracted with absorption spectroscopy, a method similar to the one used by the NACA group. The dye mass from each disk was divided by the disk area, and the reflectance of each disk was normalized with the reflectance of the white blotter paper. The results are plotted in Fig. 6. Also plotted in Fig. 6 are corresponding results obtained from Eq. (8), with assumed values for  $K^*t$ ,  $S^*t$ , and  $R_g$ . The agreement between the analytical and experimental curves is good and indicates that diffuse reflection of laser light from the dye-blotter combination can be approximated by the Kubelka-Munk model. The experimental curve shown in this figure was used to reduce all of the 1985 test data.

## Automated Data Reduction System

An automated data processing system was developed to reduce the large number of strips produced by the wind-tunnel tests. A block diagram of the automated instrument is presented in Fig. 7. Details of the design aspects of the instrument are given in Ref. 5. The data processing system consists of a laser reflectometer and a digital data acquisition system. A brief description of the system follows.

The main components of the reflectometer are a red He-Ne laser used to scan the blotter strips, a rotating drum for mounting the blotter strips, a convergent lens for collecting the reflected light, and a photodetector that converts the reflected light collected by the lens into a voltage ( $V_1$ ) that is stored for further analysis. A splitter glass plate and another

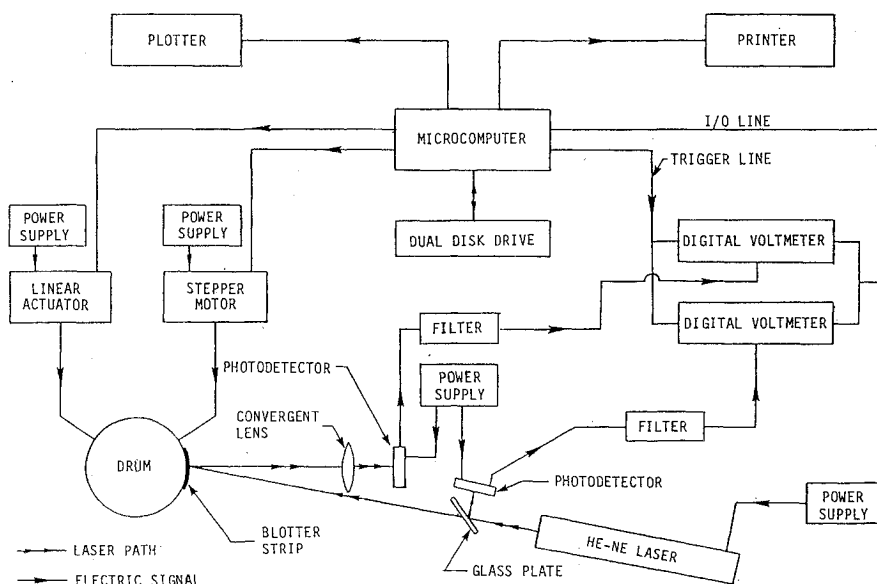


**Fig. 7** Block diagram of automated data reduction system.

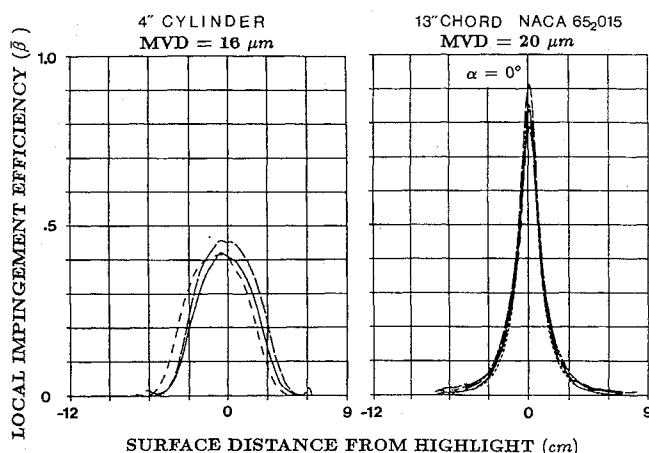


Fig. 8 Test repeatability data for a 4-in. cylinder and a NACA 652015 airfoil.

photodetector are also shown and are used to monitor fluctuations in laser output. The voltage ( $V_2$ ) from the second photodetector is also stored and is used in the data analysis.

A digital data acquisition system was also developed to control the operation of the reflectometer and to analyze and plot the data. The main components of this system are a desk top computer with two disk drives, a plotter and a printer, and two voltmeters for monitoring the voltages from the photodetectors. Appropriate software was also written for the analysis of the data.

The data reduction system is completely portable and can be taken to the test site for on-line data reduction.

#### Data Reduction Process

The reduction of the impingement data is performed in two main steps. During the first step, reflectivity values are extracted from the dyed blotter strip and are stored in the form of voltages on disk. During the second step, the reflectivity values are transformed into plots of impingement efficiency vs surface distance measured with respect to some reference point on the model.

To extract the impingement data from a single blotter strip, the strip is mounted on the drum of the laser reflectometer and three horizontal scans are obtained. For each scan, the voltages  $V_1$  and  $V_2$  from the two photodetectors are recorded and stored on disk. The reflectometer takes 47 reflectivity readings per inch of each horizontal scan at equal space intervals.

The process of transforming reflectivity into a plot of impingement efficiency vs surface distance involves the following steps.

1) The raw reflectivity values are divided by the reflectivity of the bare blotter paper to obtain normalized reflectivity data. The following equation is used for each data point of the dyed blotter paper:

$$R_{\text{norm}} = [(V_1/V_2)_{\text{DyedBlotterPaper}}] / [(V_1/V_2)_{\text{BareBlotterPaper}}] \quad (9)$$

Note that  $(V_1/V_2)_{\text{BareBlotterPaper}}$  is the average of 1000 data points measured on a reference blotter strip.

2) The normalized reflectivity data are converted into dye mass per unit area using the laser calibration curve.

3) The impingement efficiency value for each data point recorded is obtained from the following equation:

$$\bar{\beta} = \frac{\text{dye mass per unit area corresponding to a given data point}}{\text{average mass per unit area of reference collector}} \times \bar{\beta}_{\text{Collector}} \quad (10)$$

This equation is valid if the collector and the model have been exposed to sprays of identical duration, as is the case here.

All collector strips were analyzed prior to the analysis of the test model strips. Each collector strip is scanned and an average mass per unit area is calculated for the strip. This value is used as the denominator in Eq. (10). The value of  $\bar{\beta}_{\text{Collector}}$  depends on the MVD of the spray cloud and on cloud droplet distribution. The MVDs of the spray clouds used in the current tests are 16  $\mu\text{m}$  and 20  $\mu\text{m}$ . The corresponding theoretical collector efficiency values are 0.86 and 0.89.

#### Results and Discussion

In this section the repeatability of the dye tracer method and the accuracy of the data reduction method are discussed. Some experimental results are also presented.

#### Dye Tracer Method

The dye tracer method has been validated by the NACA tests performed in the 1950s. The present method retained most of the features of the NACA technique, with improvements in the measurement of droplet size and distribution. In addition, the present method uses local LWC values instead of a single average value. This should increase the accuracy of the experimental data because it reduces the effect of cloud nonuniformity.

The dye tracer method is sensitive to a number of test parameters which are subject to small statistical variations. Examples of such parameters include wind-tunnel relative humidity, which affects droplet evaporation and, therefore, droplet size, flowfield unsteadiness, spray system performance, and tunnel turbulence. It is very difficult and time consuming to precisely control such test variables. A more practical approach is to reduce their effect on the experimental data by averaging repeated test runs. The repeatability of the dye tracer method is determined by comparing the data from each run to the average of all repeated runs. Figure 8 shows typical repeatability results from the 1985 tests. In all cases, repeatability is better than  $\pm 10\%$ , which is acceptable considering the nature of the experiment.

Droplet size and distribution were provided by NASA and were obtained using a laser droplet sizing instrument. These measurements were made using a single standard IRT nozzle and were obtained for air and water pressure ratios similar to the ones used in the actual tests. The droplet data obtained for the single nozzle cloud are assumed to apply to the 12 nozzle spray cloud used in the IRT. Clearly, all 12 nozzles are not identical, and small variations in the spray cloud produced by each nozzle are expected. However, the present droplet results are believed to be more reliable than the ones obtained by the NACA group. The method used by the NACA group for determining droplet size was based on matching experimental trajectory data for cylinders and 36.5% symmetrical Joukowski airfoils with theoretical trajectory results.<sup>1,2</sup> The theoretical trajectories were obtained assuming a Langmuir "D" distribution<sup>10</sup> for the spray cloud. The NACA droplet size data are estimates whose accuracy depends on a number

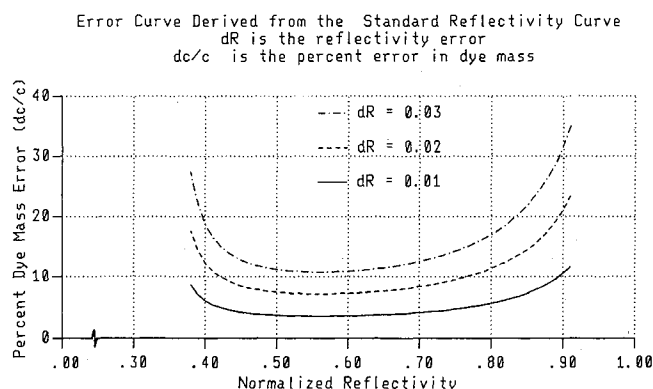


Fig. 9 Plot of  $dC/C$  as a function of normalized reflectivity.



of factors. These factors include the quality of the flow about the Joukowski airfoils, the accuracy of the method used to extract the impingement data, the assumed droplet distribution used in the theoretical calculations, the limitations of the analytical method for calculating impingement efficiency, and adjustments made to the droplet data.

#### Data Reduction Method

The repeatability and accuracy of the laser reflectance method depends on the accuracy of the laser reflectance calibration curve, the stability of the laser output power, the uniformity of blotter paper composition, the degree of dye penetration into the blotter paper, and the dye concentration range over which data are collected. A discussion of these factors follows.

The dye concentration values for the data points used in defining the laser reflectance calibration curve were obtained by absorption spectroscopy. The accuracy of this method was verified by analyzing several samples of dye solution of known concentrations. These concentrations were in the range of 200–500 mg of dye per liter of water. Absorption spectroscopy reproduced the concentrations of the sample solutions accurate to within 0.6 mg/l (i.e.,  $\pm 0.3\%$ ). To further validate the calibration method, groups of dyed blotter samples with nearly identical reflectance values were produced and analyzed by absorption spectroscopy. Results from this test are shown in Table 1. The relation between normalized reflectance and dye mass is monotonic; dye mass per unit area increases as reflectance is decreased. The results of Table 1 can be used to determine an estimate for the uncertainty in the calibration curve. Upon close examination of the data, it is seen that in some cases blotter samples with identical reflectivity values differ in dye mass by less than 2% from the average mass. Also, samples for which absorption spectroscopy produced identical dye concentrations differ in reflectivity by less than 2% from the average reflectivity. It is reasonable to conclude that the uncertainty in the calibration curve is of the order of 2%.

During the early stages of the development of the laser reduction method, it was found that the output light intensity of the laser beam varied significantly over long periods of time. Since the light reflected from the blotter paper is a direct function of the incident light, the laser fluctuations must be monitored and taken into account during the data reduction. First, the He-Ne laser used in the preliminary studies was replaced with a polarized He-Ne laser. Experience indicates that polarized lasers give a more stable output. Second, optical feedback was incorporated to monitor any remaining fluctuations in laser power. During the data reduction, the effect of laser power fluctuations is essentially eliminated by using the

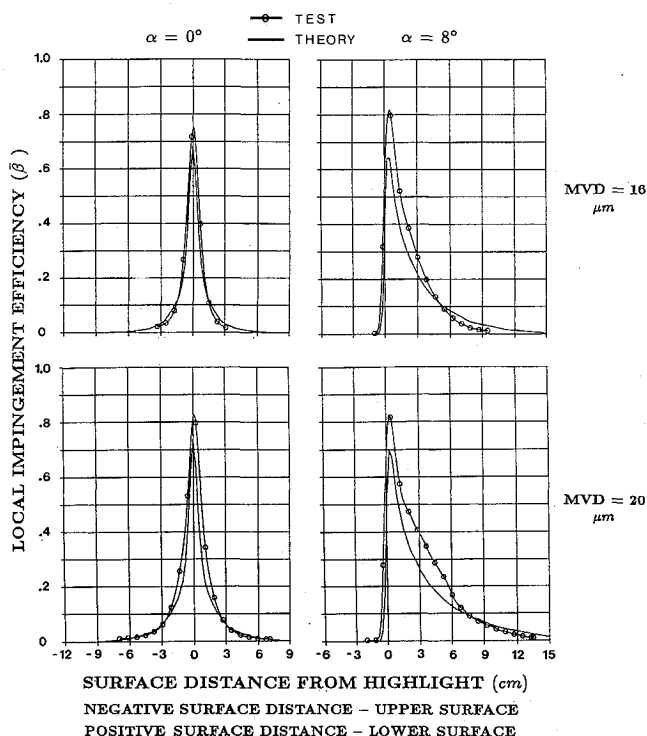


Fig. 11 Impingement data for a NACA 652015 airfoil at  $\alpha = 0$  deg,  $V_\infty = 181$  mph.

ratio of the collected signal to the feedback signal, as explained in the third section. The optical feedback design was tested by scanning a reference bare blotter strip a number of times over a period of several months. Each time, 400 reflectance measurements were obtained and the average of the 400 data points was evaluated. The standard deviation of these averaged reflectance values was found to be  $\pm 0.3\%$ .

The uniformity of the reflectivity of an unsprayed (bare) piece of blotter paper was measured by scanning 200 points at five horizontal locations. The variation in reflectance was  $\pm 1.3\%$  from the average value, based on 1000 ( $5 \times 200$ ) reflectance measurements. This variation in reflectance is due to the roughness of the paper itself and due to variation in the composition of the blotter paper.

Penetration of dye into the blotter paper should be avoided because the data reduction is based on surface reflectance measurements. This was accomplished by keeping the spray time as short as possible. A series of tests were performed to establish the optimum spray time for each droplet size used in the actual impingement experiments. During these tests, blotter strips were exposed to sprays of various time durations. After each test, the penetration of dye into the paper was examined using a microscope. Spray times of the order of 3–5 s produced penetrations of the order of 10% of the blotter thickness. This level of penetration is acceptable and does not affect the quality of the data.

The preceding discussion indicates that the error in measuring reflectance is of the order of 2%. The corresponding error in extracting the dye mass per unit area of blotter paper needs to be determined. Let the absolute error in reflectance be  $dR$ . The absolute error in dye mass per unit area  $dC$  is a function of  $R$  and  $dR$ , where  $R$  is the normalized reflectance. For  $R$  values close to 1, a given  $dR$  has a small  $dC$  associated with it. Near the low end of the reflectivity axis, e.g., for  $R$  values near 0.3, the same value of  $dR$  produces a large  $dC$ . In both cases, however, the percent error in dye mass per unit area ( $dC/C$ ) is large. In the first case,  $dC$  is small but  $C$  is also very small, and so the ratio  $dC/C$  is large. In the second case,  $dC$  is large while

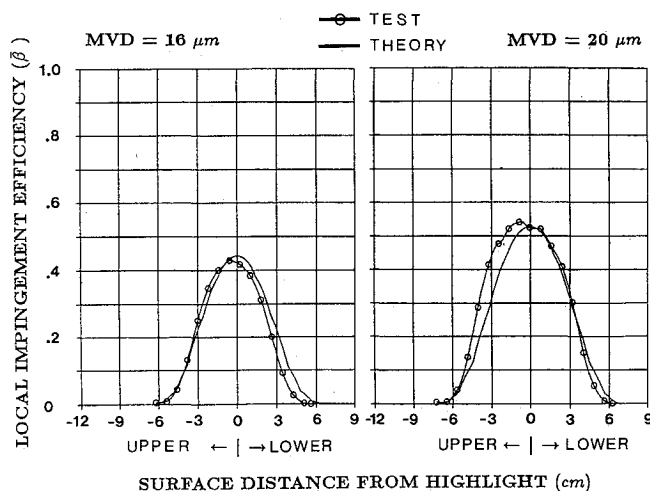


Fig. 10 Impingement data for a 4-in.-diam cylinder;  $V_\infty = 180$  mph.



Table 1 Laser reflectance calibration data

| Dye mass,<br>$\mu\text{g}/\text{cm}^2$ | Normalized<br>reflectance | Dye mass,<br>$\mu\text{g}/\text{cm}^2$ | Normalized<br>reflectance |
|--|---------------------------|--|---------------------------|
| 0.160                                  | 0.849                     | 1.168                                  | 0.382                     |
| 0.162                                  | 0.835                     | 1.168                                  | 0.371                     |
| 0.320                                  | 0.694                     | 1.531                                  | 0.364                     |
| 0.324                                  | 0.692                     | 1.535                                  | 0.362                     |
| 0.624                                  | 0.524                     | 2.230                                  | 0.311                     |
| 0.624                                  | 0.519                     | 2.250                                  | 0.310                     |
| 0.797                                  | 0.447                     | 2.980                                  | 0.265                     |
| 0.803                                  | 0.437                     | 3.138                                  | 0.261                     |
| 1.121                                  | 0.396                     | 3.335                                  | 0.232                     |
| 1.151                                  | 0.396                     | 3.355                                  | 0.228                     |

$C$  has some finite size, and so the ratio  $dC/C$  remains large. Between these extremes, there is a region where  $dC/C$  is reduced to a minimum. This region of low values in  $dC/C$  corresponds to a certain range of absolute normalized reflectivity. This range of reflectivity is determined by differentiating  $R$  with respect to  $C$  and plotting  $dC/C$  as a function of  $R$ . The calibration curve is first approximated with cubic splines, and the differentiation is performed numerically. Plots of  $dC/C$  vs  $R$  for  $dR = 0.01$ ,  $0.02$ , and  $0.03$  are given in Fig. 9. To maintain, for example, the percent error in the measurement of dye mass per unit area to less than 10%, assuming 1% error in normalized reflectance (i.e.,  $dR = 0.01$ ), the normalized reflectance of the dyed blotter paper must be in the range of 0.31–0.87. To obtain reflectance values within the required range, the concentration of the dye solution and the duration of the spray must be chosen carefully.

### Experimental Results

Experimental impingement data for a 4-in.-diam cylinder and a NACA 65<sub>2</sub>015 airfoil at two angles of attack are presented for the purpose of validating the experimental method and the new data reduction method. These data were obtained during the 1985 tests. Results for these geometries are also available, from tests performed by the NACA group in the 1950s,<sup>1,2</sup> and have been used to validate a number of two-dimensional trajectory codes.

The present experimental data cannot be compared directly with the NACA experimental data because of differences in spray cloud MVDs and distributions. Therefore, a two-dimensional trajectory computer code,<sup>6</sup> which has been validated with the NACA experimental data, was used to test the validity of the new impingement results. Analytical impingement data were obtained from this code for the 4-in.-diam cylinder and for the NACA 65<sub>2</sub>015 for all flow and spray cloud conditions. The analytical and the recently obtained experimental data are compared in Figs. 10 and 11.

The main features of the impingement curves presented in these figures are the overall shape of the curve, the magnitude and location of peak impingement efficiency, and the extent of the impingement limits. The overall agreement between the analytical and the present experimental impingement curves, shown in Figs. 10 and 11, with regard to these features is good. The present experimental data have also been compared to results from several other two-dimensional computer codes, and good agreement has been demonstrated.<sup>11</sup>

Analytical impingement data for thin airfoils at small angles of attack can be used as a reference for testing experimental methods. This is because the flow in such simple test cases is nearly ideal, and the impingement region is usually limited to the area very close to the leading edge. It is difficult to precisely determine the accuracy of such calculations. However, by comparing the analytical and experimental data for air-

foils, and by examining the repeatability of the test data, estimates for the uncertainty in the experimental results can be obtained.

The uncertainty in the experimental data obtained by the NACA group is  $\pm 10\%$  and in some cases  $\pm 25\%$ , as discussed in Refs. 1 and 2. In most cases, the present experimental data agree with the analytical data to within  $\pm 10\%$  for the configurations presented. It is reasonable to assume that the impingement data for the airfoils and engine inlets studied during the present program and reported in Ref. 5 have a similar degree of uncertainty.

### Summary

The dye tracer technique presented can be applied to arbitrary geometries for obtaining water droplet impingement characteristics. A new method for measuring local LWC was developed and is believed to be more accurate than other methods used previously. Experimental data show that the repeatability of the method is better than 10%. The new data reduction method presented is accurate and repeatable. The method is at least an order of magnitude more efficient than the method of colorimetric analysis and is capable of much higher resolution. Experimental impingement data presented for a 4-in.-diam cylinder and a NACA 65<sub>2</sub>015 airfoil show good agreement with analytical data obtained from a two-dimensional computer code that has been validated using the NACA results.

### Acknowledgments

Funding support was provided by the FAA and NASA through NASA Lewis Research Grant NAG-3-566. The authors would like to thank the project technical monitors J. T. Riley of the FAA, and R. J. Shaw and J. J. Reinmann of NASA Lewis Research Center. The support of G. W. Zumwalt of Wichita State University and of J. Newton, C. S. Bidwell, and W. Olsen of NASA Lewis Research Center is gratefully acknowledged.

### References

- <sup>1</sup>Von Glahn, U. H., Gelder, T. F., and Smyers, W. H., "A Dye-Tracer Technique for Experimentally Obtaining Impingement Characteristics of Arbitrary Bodies and a Method for Determining Droplet Size Distribution," NACA TN 3338, March 1955.
- <sup>2</sup>Gelder, T. F., Smyers, W. H., and Von Glahn, U. H., "Experimental Droplet Impingement on Several Two-Dimensional Airfoils with Thickness Ratios of 6 to 16 Percent," NACA TN 3839, Dec. 1956.
- <sup>3</sup>Lewis, J. P., and Ruggeri, R. S., "Experimental Droplet Impingement on Four Bodies of Revolution," NACA TN 4092, Dec. 1957.
- <sup>4</sup>Gelder, T. F., "Droplet Impingement and Ingestion by Supersonic Nose Inlet in Subsonic Tunnel Conditions," NACA TN 4268, May 1958.
- <sup>5</sup>Papadakis, M., Elangovan, R., Freund, G. A., Jr., Breer, M. D., Zumwalt, G. W., and Whitmer, L., "An Experimental Method for Measuring Droplet Impingement Efficiency on Two- and Three-Dimensional Bodies," NASA CR 4257, DOT/FAA/CT-87/22, Nov. 1989.
- <sup>6</sup>Breer, M. D., and Seibel, W., "Particle Trajectory Computer Program-User Manual," Boeing Document D3-9655-1, Dec. 1976.
- <sup>7</sup>Wendlandt, W. W., and Hecht, H. G., *Reflectance Spectroscopy*, Interscience, New York, 1966.
- <sup>8</sup>Kubelka, P., "New Contributions to the Optics of Intensely Light-Scattering Materials—Part I," *Journal of the Optical Society of America*, Vol. 38, May 1948.
- <sup>9</sup>Frei, R. W., and MacNeil, J. D., "Diffuse Reflectance Spectroscopy in Environmental Problem-Solving," Chemical Rubber Co. Press, Cleveland, OH, 1973.
- <sup>10</sup>Langmuir, I., and Blodgett, K. B., "A Mathematical Investigation of Water Droplet Trajectories," Army Air Forces TR No. 5418, Feb. 1946.
- <sup>11</sup>NASA Lewis Droplet Trajectory Workshop, NASA Lewis Research Center, Cleveland, OH, Oct. 15, 1987.